Wave Propagation Characteristics of a Reactively Loaded Microstrip

Karam Michael Noujeim, Member, *IEEE*

Anritsu Company, Morgan Hill, CA, 95037, USA

***Abstract* — The characteristics of wave propagation along a reactively loaded microstrip operating in its first higher-order mode are investigated by means of the transverse-resonance and two-dimensional finite-difference time-domain techniques. It is found that the phase velocity along the microstrip and the cutoff frequency of its first higher-order mode are functions of the reactive-load value. These effects are used to design fixed-frequency continuously beam-steerable leaky-wave antennas, and antennas with a continuously adjustable operating frequency range.**

I. INTRODUCTION

The leakage mechanism of a microstrip operating in its first higher-order mode (EH_1) has been used successfully in the design of microstrip leaky-wave antennas [1,2]. Recently, applications employing this microstrip as a radiating element have appeared in the literature, and have dealt with fixed-frequency continuous main-beam steering [3,4], dual-beam frequency scanning [5], and phased arrays with a reconfigurable aperture [6].

In [3,4], the leaky-wave microstrip was divided into a number of regular sections along the direction of wave propagation. Identical varactor diodes were used to connect adjacent sections, so as to form a finite-length periodic structure. By reverse-biasing the series-connected varactor diodes between 0 and −900 volts, a 60-degree scan range was achieved at 5.2 GHz both theoretically and experimentally.

Interest in reducing the DC-voltage requirement of the fixed-frequency continuously beam-steerable periodic microstrip introduced in [3,4] without resorting to varactors mounted in shunt through the dielectric, prompted the author to investigate the propagation characteristics of waves traveling along a new structure, the reactively loaded microstrip. The theoretical details of this investigation will be presented in the sections that follow, and will focus on the first higher-order mode of operation.

II. ANALYSIS

A. Propagation-Constant Calculations

A cross-sectional view of the microstrip under investigation is shown in Fig. 1(a). A reactive sheet of width $\delta<<h$, and surface reactance $X_s=-1/(\omega C)$ (Ω/square) lies along the bisecting line of the top $2d$-wide conductor. Here, the dielectric thickness h is chosen such that surface-wave modes beyond the TM_0 mode are cutoff.

The structure shown in Fig. 1(a) supports hybrid modes whose complex propagation constants may be found by application of the transverse-resonance technique [2,7,8]. An essential ingredient to the success of this technique is an accurate prediction of Z_h, the impedance of the open end located at $x=\pm d$.

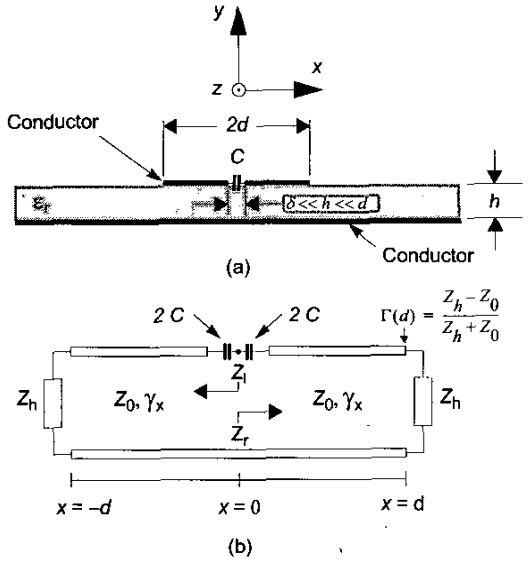

Fig. 1. A reactively loaded microstrip. (a) Cross-sectional view. (b) A transmission-line model for wave propagation along the x direction.

In [2], a Wiener-Hopf technique was used to find the impedance of the open end [9], which resulted in an accurate prediction of the propagation constants of the modes supported by an unloaded microstrip. Here, the open-end impedance is found by making use of the two-dimensional finite-difference time-domain (2D FDTD) technique [10], in which use is made of a twelve-cell-thick perfectly matched layer (PML) [11] on the top, left, and

0-7803-7695-1/03/$17.00 © 2003 IEEE

right walls as shown in Fig. 2. A y-polarized Gaussian pulse generated by a voltage source located between the conducting bottom wall and the top strip at $x=x_g$ is incident on the open end. The ratio of the Fourier transforms of the y-polarized electric field and z-polarized magnetic field at the open end ($x=x_h$) provides Z_h.

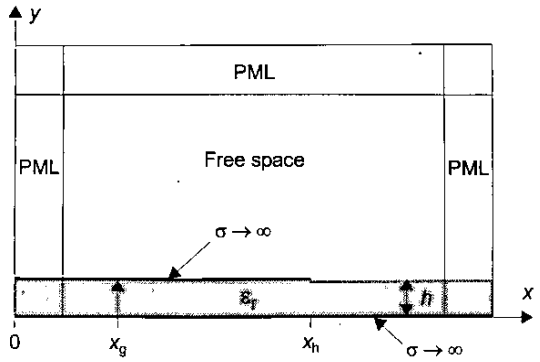

Fig. 2. 2D-FDTD setup for calculating the impedance of the open end located at $x = x_h$.

The stage is now set for applying the transverse-resonance technique [2,7,8] to the circuit shown in Fig. 1(b). This results in the following equation for the complex propagation constant along the x direction:

$$\gamma_x = \frac{j}{2d}\left(\ln\left|\frac{-jX_s/2+Z_0}{-jX_s/2-Z_0}\right| - \ln|\Gamma(d)| + j(\tau-\phi+2n\pi)\right) \qquad (1)$$

$n = 0, 1, 2, \ldots$

where n is the propagation-mode index, Γ is the reflection coefficient, Z_0 is the TEM wave impedance in a dielectric having a relative constant ε_r, $\phi = Arg(\Gamma(d))$, and

$$\tau = Arg\left(\frac{-jX_s/2+Z_0}{-jX_s/2-Z_0}\right)$$

With γ_x known, the complex propagation constant γ_z along the direction of wave propagation may be calculated readily using

$$\gamma_z = \sqrt{k_s^2 - \gamma_x^2}, \qquad (2)$$

where k_s is the propagation constant of the TM_0 surface-wave mode, assumed by a proper choice of h to be the only propagating one. Eqs. (1) and (2) show the dependence of γ_z on the surface reactance X_s, and thus on the reactive loading. The extent of this dependence and its implications will be explored next by means of two antenna examples.

B. Dependence of γ_z on the Value of the Reactive Load

The analysis technique described in Section A was used to calculate the normalized leakage and propagation constants of the EH_1 mode propagating along a reactively loaded microstrip. The results are shown in Figs. 3 and 4 for different values of $C \in [0.05, 1.0]$ pF. Here, the microstrip dielectric constant $\varepsilon_r=2.2$, the dielectric thickness $h=0.127$ mm, and the strip width $2d=3.5$ mm.

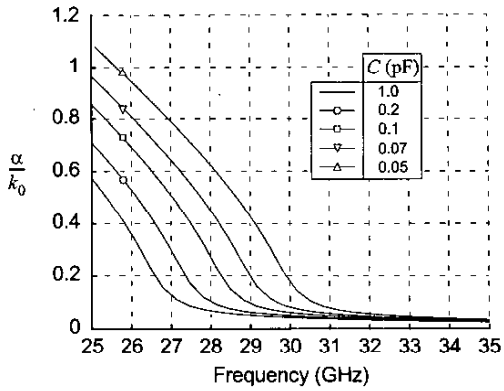

Fig. 3. The normalized leakage constant α/k_0 of the EH_1 mode in a reactively loaded microstrip with $\varepsilon_r = 2.2$, $h = 0.127$ mm, $2d = 3.5$ mm, and $C \in [0.05, 1.0]$ pF. The free-space wave number is denoted by k_0.

Figure 4 shows that an increasing value of C has the effect of making the microstrip waveguide appear wider, and causes a downward shift in the cutoff frequency of the EH_1 mode. Here, a shift of about 3 GHz in the cutoff frequency of the EH_1 mode is observed as C is increased from 0.05 to 1 pF. Figure 4 also shows that at a constant frequency f, a continuous increase in the value of C is accompanied by a continuous decrease in the phase velocity along the microstrip, and thus a continuous movement of the main-beam maximum toward endfire.

For a microstrip of length L, the H-plane power-gain pattern may be calculated by treating the microstrip as a line source [12], and by making use of the element factor of an x-directed infinitesimal current element lying on a grounded dielectric slab of infinite extent [13]. For a microstrip of length $L=4.9\ \lambda_0$, where λ_0 is the free-space wavelength at $f=30$ GHz, this approach results in the normalized H-plane power-gain patterns shown in Fig. 5 for different values of $C \in [0.05, 1.0]$ pF. This choice of L ensures that at least 90% of the input power is radiated by the time the EH_1 wave reaches the end of the microstrip.

Figure 5 shows that as C is decreased from 1 to 0.05 pF, the main-beam maximum scans a 35° range at a constant frequency f=30 GHz. This is accompanied by a widening of the main beam, and is due mainly to the fact that the leakage constant α shown in Fig. 3 increases as C is decreased, resulting in a shorter radiating aperture.

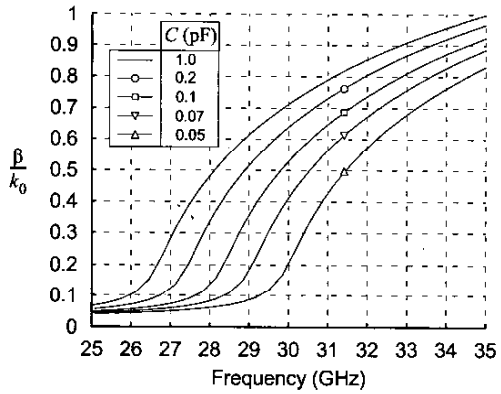

Fig. 4. The normalized phase constant β/k_0 of the EH_1 mode in a reactively loaded microstrip with ε_r= 2.2, h = 0.127 mm, $2d$ = 3.5 mm, and $C \in$ [0.05, 1.0] pF.

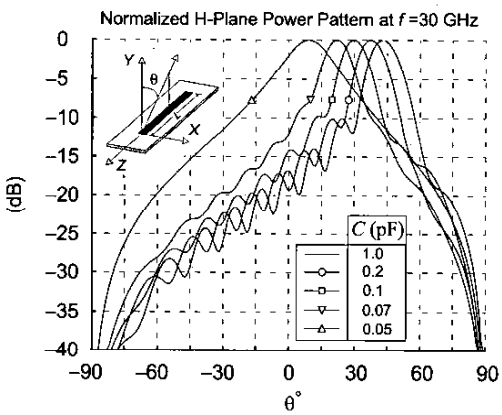

Fig. 5. The normalized H-plane power-gain patterns of the 4.9-λ_0-long reactively loaded microstrip for ε_r = 2.2, f = 30 GHz, and $C \in$ [0.05, 1.0] pF. The normalization factor for each of the patterns is its maximum power gain.

An analysis similar to that performed earlier is used in the case of a microstrip with a dielectric constant ε_r=3.78, thickness h=0.127 mm, and strip width $2d$=2.67 mm. The results are shown in Figs. 6, 7, and 8 for different values of $C \in$ [0.05, 1.0] pF. Here, a 64° main-beam scan range is achieved at a constant frequency f=30 GHz, and is accompanied by a shift of about 4 GHz in the cutoff frequency of the EH_1 mode.

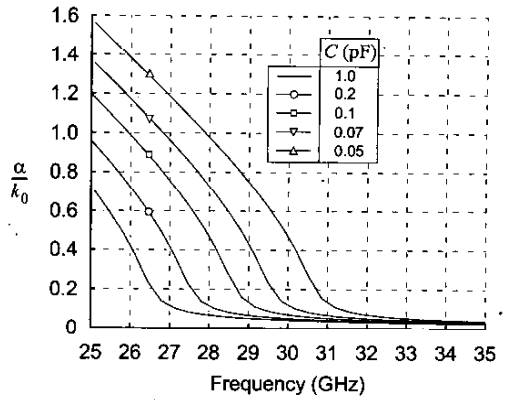

Fig. 6. The normalized leakage constant α/k_0 of the EH_1 mode in a reactively loaded microstrip with ε_r= 3.78, h = 0.127 mm, $2d$ = 2.67 mm, and $C \in$ [0.05, 1.0] pF.

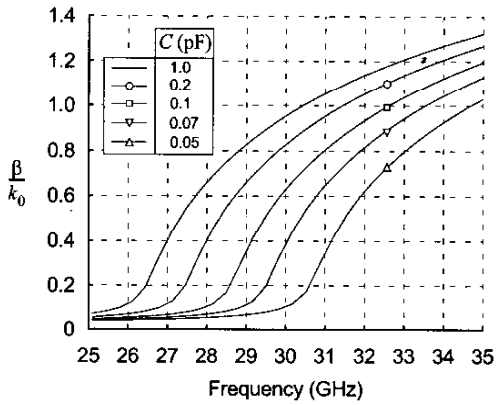

Fig. 7. The normalized phase constant β/k_0 of the EH_1 mode in a reactively loaded microstrip with ε_r= 3.78, h = 0.127 mm, $2d$ = 2.67 mm, and $C \in$ [0.05, 1.0] pF.

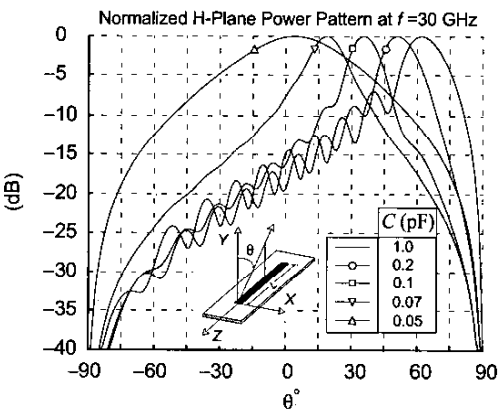

Fig. 8. The normalized H-plane power-gain patterns of the 4.9-λ_0-long reactively loaded microstrip for ε_r= 3.78, f = 30 GHz, and $C \in$ [0.05, 1.0] pF. The normalization factor for each of the patterns is its maximum power gain.

The reactive loading can take the form of a ferroelectric film such as BST [14]. Alternatively, a periodic array of ferroelectric strips placed in shunt across the microstrip center gap can be used, and would result in antennas with a higher radiation efficiency. Another form of loading is a periodic array of varactors (Schottky or MEMS [15]) requiring a reverse-bias voltage range that is much smaller than that used in [3,4], due to the shunt mounting of the varactors across the microstrip center gap.

III. CONCLUSIONS

In conclusion, it was found that the phase velocity along a reactivley loaded microstrip operating in its first higher-order mode may be varied continuously at constant frequency by varying its surface reactance. This effect can be used to achieve fixed-frequency continuous main-beam steering.

It was also found that a change in the surface reactance is accompanied by a shift in the cutoff frequency of the first higher-order mode. This effect is similar to changing the width of the microstrip waveguide, and may be used in the design of antennas with a continuously adjustable operating frequency range.

It is interesting to note that the reactively loaded microstrip may be used as a variable-delay transmission line when operated below f_{c1}, the cutoff frequency of its first higher-order mode. On the other hand, when loaded periodically with reverse-biased Schottky varactors, and driven in large-signal mode at frequencies that are much smaller than f_{c1}, the structure may be used as a nonlinear transmission line for the generation of nonlinear waves such as electrical shock waves and solitons [16].

REFERENCES

[1] W. Menzel, "A new traveling-wave antenna in microstrip," *Arch. Elektron. Übertragungstech.*, vol. 33, no. 4, pp. 137-140, April 1979.

[2] A. A. Oliner and K. S. Lee, "Microstrip leaky-wave antennas," *1986 IEEE International Antennas and Propagation Symposium Digest*, Philadelphia, PA, pp. 443-446, June 8-13, 1986.

[3] K. M. Noujeim, "Fixed-frequency beam-steerable leaky-wave antennas," Ph.D. Thesis, University of Toronto, Ontario, Canada, 1998.

[4] K. M. Noujeim and K. G. Balmain, "Fixed-frequency beam-steerable leaky-wave antennas," XXVIth General Assembly, International Union of Radio Science (URSI), Aug. 1999.

[5] C.-J. Wang, C. F. Jou, and J.-J Wu, "A novel two-beam scanning active leaky-wave antenna," *IEEE Transactions on Antennas and Propagation*, vol. 47, no. 8, Aug. 1999.

[6] J. Sor, C.-C. Chang, Y. Qian, and T. Itoh, "A reconfigurable leaky-wave/patch microstrip aperture for phased-array applications," IEEE Transactions on Microwave Theory and Techniques, vol. 50, no. 8, Aug. 2002.

[7] N. Marcuvitz, "On field representations in terms of leaky modes or eigenmodes," *IRE Transactions on Antennas and Propagation*, vol. AP-4, no. 3, pp. 192-194, July 1956.

[8] S. V. Zaitsev and A. T. Fialkovskii, "Edge effects in strip structures with an arbitrary grazing angle of the wave. Waves in a microstrip waveguide," *Radio Phys. Quant. Electron.*, vol. 24, no. 9, pp. 786-791, Sept. 1981.

[9] D. C. Chang and E. F. Kuester, "Total and partial reflection from the end of a parallel-plate waveguide with an extended dielectric slab," *Radio Science*, vol. 16, no. 1, pp. 1-13, Jan.-Feb. 1981.

[10] K. S. Yee, "Numerical solution of initial boundary value problems involving Maxwell's equations in isotropic media," *IEEE Transactions on Antennas and Propagation*, vol. 14, pp. 302-307, 1966.

[11] J.-P. Berenger, "A perfectly matched layer for the absorption of electromagnetic waves," *Journal of Computational Physics*, vol. 114, pp. 185-200, 1994.

[12] W. L. Stutzman and G. A. Thiele, *Antenna Theory and Design*, John Wiley & Sons, Inc., 605 Third Ave., New York, NY 10158-0012, pp. 137-141 and 173-174, 1981.

[13] P. Perlmutter, S. Shtrikman, and D. Treves, "Electric surface current model for the analysis of microstrip antennas with application to rectangular elements," *IEEE Transactions on Antennas and Propagation*, vol. AP-33, no. 3, pp. 301-311, March 1985.

[14] O. Vendik, I. Mironenko, and L. Ter-Martirosyan, "Superconductors spur application of ferroelectric films," *Microwaves & RF*, vol. 33, no. 7, pp. 67-70, July 1994.

[15] N. S. Barker, and G. M. Rebeiz, "Distributed MEMS true-time delay phase shifters and wideband switches," *IEEE Transactions on Microwave Theory and Techniques*, vol. 46, no. 11, Nov. 1998.

[16] M. J. W. Rodwell *et al.*, "Active and nonlinear wave propagation devices in ultrafast electronics and optoelectronics," *IEEE Proceedings*, vol. 82, no. 7, pp. 1037-1058, July 1994.